

# Research Journal of Pharmaceutical, Biological and Chemical Sciences

## Potency Of Titanium Dioxide Nanoparticles On Skin Wound Healing In Rats.

Aziza M Amer<sup>1\*</sup>, Ahmed I Abd El Maksoud<sup>2</sup>, Mohamed A Abdeen<sup>1</sup>, Amera Hamdy<sup>3</sup>,  
Hana A Mabrok<sup>4</sup>, Mohamed M Amer<sup>1</sup>, and Ahmed A El-Sanousi<sup>1</sup>.

<sup>1</sup> Faculty of Veterinary Medicine, Cairo University, Egypt

<sup>2</sup> Genetic Engineering and Biotechnology Research Institute (GBRI), University of Sadat City, Egypt.

<sup>3</sup> Collage of Biotechnology, Misr University for Science and Technology (MUST), Egypt.

<sup>4</sup> Animal Health Research Institute, Dokki, Giza, Egypt

### ABSTRACT

Wound is as damage or disruption to the normal anatomical structure and function, it can range from a simple break in the epithelial integrity of the skin or it can be deeper, extending into subcutaneous tissue. Titanium dioxide nanorods (TiO<sub>2</sub>-NRs) were biosynthesized abundantly and confirmed its rod shape with the dimensions of 244-246 nm length and 532-649 nm diameter, respectively. Chicken embryo chorioalantoic membrane (CAM) vascular assay was used in studying angiogenesis of prepared TiO<sub>2</sub>-NRs and proved that both 10 and 20 µg/0.2ml showed good angiogenesis effect as evaluated by microscopical examination for collateral proliferation of blood vessels and histological examination of the treated fertile chicken's eggs CAM. Also, the dose 20 µg/0.2ml TiO<sub>2</sub>-NRs showed activity of angiogenesis better than 10 µg/0.2ml TiO<sub>2</sub>-NRs. The effects of different concentration TiO<sub>2</sub> nanoparticles on wound healing in Albino rats were used for evaluating the macroscopic and the microscopic effect of skin wound dressing on angiogenesis and wound healing. The animals of un-treated treated by phenytoin as standard healing promoting drug (control positive) drug, 10 µg/200 µl and 20 µg/200 µl groups showed thickening of epidermis at its cut edges. The dermis near the excision area was rich in polymorphonuclear cells which mainly represent the inflammatory cells. The obtained results proved that dressing with TiO<sub>2</sub>-NRs (10 and 20 µg/ 200 µl) resulted in good angiogenesis with formation of new capillaries and endothelial cells proliferation in skin wounds at 3, 5 and 7 days of treatment as well as rapid wound healing from 3 to 14 days of treatment as compared with control negative and phenytoin spray. Dressing with 20 µg/0.2ml gave the best result. It can be concluded that the wound dressing with TiO<sub>2</sub>-NRs showed promoting effect on wound healing. It is advisable to be used with other medications to cut short the time of wound healing and further investigation has to be done to clarify the exact mechanism of TiO<sub>2</sub>-NRs promotes wound healing.

**Keywords:** TiO<sub>2</sub>, Nanorods, Angiogenesis, CAM, wound healing, albino rats, phenytoin, histological change.

*\*Corresponding author*

## INTRODUCTION

Titanium dioxide (TiO<sub>2</sub>) is a natural oxide of the element titanium with negligible biological effects and of low toxicity. Nanoparticles (NPs); are very small materials on the nanometer scale; 1,000,000,000 nanometers in one meter; the abbreviation for a nanometer is nm. Nanometer is nm, nanoparticles in size from (1 nm: 100 nm) nanoparticles are classified based on the dimension of their structure [1]. TiO<sub>2</sub> nanoparticles (TiO<sub>2</sub>-NPs) are used extensively in food products and in a wide range of pharmaceutical products and cosmetics as sunscreens and toothpastes [2]. Therefore, human exposure may occur through ingestion, dermal penetration and inhalation route, during both the manufacturing process and use [3].

Rutile TiO<sub>2</sub> nanorods (TiO<sub>2</sub>-NRs) was synthesis via the best method which is direct hydrolysis of inorganic titanium salts in aqueous solutions under hydrothermal or moderate conditions [4, 5]. It offers considerable promise in various biomedical applications as drug delivery, gene and antigen delivery [6].

In spite of the extensively use of TiO<sub>2</sub>-NPs, the biological effects and the mechanisms of cellular response are not completely understudied [7, 8]. The extent and type of cell damage depend strongly on both chemical and physical characteristics of TiO<sub>2</sub>-NPs, including size, photo-activation and crystal structure [2].

One of the most important technical challenges in the studies of angiogenesis is selection of the appropriate assay method. There are increasing numbers of in vitro and in vivo angiogenesis assays described in literature [9]. Chorioallantoic membrane (CAM) assay has been reported as an invivo assay model to study angiogenesis [10] and evaluation of drug delivery systems [11]. Hen's egg test CAM and CAM vascular assay [12].

Wound is a damage or disruption to the normal anatomical structure and function of skin. It is ranging from a simple break in the epithelium to extending into the subcutaneous tissue with damage to other structures (tendons, muscles, vessels, nerves, parenchymal organs and even bone) [13]. A physiological response to the noxious factor results in bleeding, vessel contraction with coagulation, activation of complement and an inflammatory response [14].

TiO<sub>2</sub> NPs are known to be of popular wide use due to it is cost effective, safe for humans and the environment, stable and non-carcinogenic and nontoxic [15]. TiO<sub>2</sub> NPs exist in three crystalline phases demonstrates high antimicrobial properties [16]. The antimicrobial activity of *G. zeylanica* extract to Methicillin resistant *Staphylococcus aureus* was enhanced in the presence of TiO<sub>2</sub> NPs [17]. The broad spectrum antimicrobial activity of TiO<sub>2</sub> even in the absence of photo activation has been reported [18].

Studies on healing of burn wounds in rat demonstrated the formation of a strongly adherent crust of a Nano-composite, preventing both infection and inflammation with rapid reduction of wound area as compared with untreated control. The dispersion of the TiO<sub>2</sub> was resulted in the improved regeneration of damaged tissues with considerable decrease in scar tissue formation and anomalies in skin color [17]. A significant activity of TiO<sub>2</sub> NPs was reported on wound healing in the excision wound model in Albino rats by measuring wound closure, histopathology and protein profiling. In clinical practice TiO<sub>2</sub> NPs have delivered a novel therapeutic route for wound treatment [19].

Phenytoin was found to promotes wound healing by stimulation of fibroblast proliferation, enhancing the formation of granulation tissue, decreasing collagenase activity, inhibition of glucocorticoid activity, direct or indirect antibacterial activity by affecting inflammatory cells, neovascularization [20, 21]. Phenytoin has wide antibacterial activity [20, 22].

The study amide to determine the effect of titanium dioxide nanorods (TiO<sub>2</sub>-NRs) biosynthesis in yeast on Angiogenesis of chicken embryo CAM and skin wound healing promoter rats as compared with Phenytoin as standard commercial drug.

## MATERIAL AND METHODS

### Synthesis and Characterization of rutile TiO<sub>2</sub>-NRs:

#### Synthesis of rutile TiO<sub>2</sub>-NRs:

Materials used are TiCl<sub>3</sub> (15% HCL), ethanol, D-glucose, yeast extract peptone, Na<sub>2</sub>HPO<sub>4</sub>, citric acid [23]. TiO<sub>2</sub>-NRs were synthesized by hydrolysis of TiCl<sub>3</sub> in aqueous media mixed with Albumin egg shells. In typical synthesis, 1.5 gm of Albumin egg shells aqueous suspension at room temperature in 300 ml of milli-Q water (18M Ω) then stirring for 15 min, then add 10 ml of TiCl<sub>3</sub> (15% HCL) slowly with rate (1 drop per 2 second) until color change from colorless to purple and stirring with 1500 rpm for 1 hour. and stand it for 6 days at room temperature. The precipitation was collected by centrifugation method and wash with ultrapure water several times then with absolute ethanol until the supernatant become colorless after centrifugation, and dried at room temperature and calcination at 700 C<sup>0</sup> for 90 minutes [5].

#### Characterization of TiO<sub>2</sub>-NRs:

The crystalline nature and grain size of TiO<sub>2</sub>-NRs was carried out by X-ray diffraction (XRD) pattern at 25-280C with a D8 Advance X-ray diffractometer (Bruker – Germany) with a nickel (Ni) filtered using CuKα (λ= 1.54184 Å) radiations as an X-ray source. A Fourier transform-infrared spectrum (FTIR) of sample is registered using Nicolet 6700 (Thermo scientific –USA). Morphology and size of TiO<sub>2</sub> nanoparticle were examined by field emission transmission electron microscopy (FETEM, JSM- 2100F, JEOL Inc.) at an accelerating voltage of 15Kv and 200 Kv [24].

#### Specific pathogen free (SPF) fertile eggs:

Sixty White Luhmann fertilized Specific pathogen free (SPF) chicken eggs were obtained from SPF farm Koum Oshem El-fayoum, Government, Egypt. SPF eggs were incubated in sterile incubator at 37 °C ± 0.3 °C. SPF eggs were used for studying Angiogenesis effect of TiO<sub>2</sub>-NRs on chicken embryo chorioallantoic membrane (CAM).

#### Inoculation of SPF embryos:

The used 4 days embryonated SPF chicken eggs surface were cleaned and sterilized using 70% alcohol and incubated in egg incubators at 37 °C ± 0.3 °C in a vertical position. On day 5, the egg shell was pierced with an 18 gauge needle and 200 µl of vehicle (negative control) the tested materials and incubated for further 6 day.

#### Photographing:

CAMs images were taken on a white background by Sony Cybershot DSCW55 7.2 megapixels digital camera with 5× optical zoom, resolution of 640 × 480 pixels, with 50 × magnifications and Olympus dissection microscope with 50 × magnifications.

#### Male albino rats:

A group of 60 male albino rats (200-250 g) was obtained from animal house and hygienically transferred to the laboratory. The animals was feed on commercial pellet diet, given deionized water ad libitum and kept in plastic cages in 20 ± 2 C, 50 -70 % relative humidity and 12 h light/ dark cycle. After 2 weeks acclimation, the rats were randomly divided into 4 equal groups; 15 rats each.

#### Wound dressing:

Post-operative wound dressing Pharmafix<sup>®</sup> retaining gauze and absorbent pads with hypoallergenic lot no 31/08 produced by Pharmaplast Kafer El Zayat, Egypt.

**Phenytoin spray (Standard drug):**

Phenytoin 2 % aerosol powder Healosol® each 150 ml contain 40 mg Phenytoin base manufactured by Egyptian Company for Advanced Pharmaceutical, Cairo, Egypt.

**Angiogenesis effect of TiO<sub>2</sub>-NRs:**

The Angiogenesis effect of TiO<sub>2</sub>-NRs was carried out on chicken embryo CAM [25].

**Preparation and treatment of CAM:**

Forty, 5 days old embryonated SPF chicken eggs were divided 0.2 ml solutions into 4 groups; 10 each. Embryos of groups 1-3 were inoculated with 10 µg/200 µl, 20 µg/200 µl TiO<sub>2</sub>-NRs in dimethyl sulphoxide (DMSO) and 200 µl of vehicle (vehicle control); respectively. Group 4 embryos were kept as non-injected (negative control). Injected embryos and controls were incubated and subjected for daily observation for mortalities. On day 12; 6/group were randomly selected and their CAMs were examined under stereomicroscope for collateral proliferation of blood vessels and photographed.

**Evaluating the vasoproliferative response by semiquantitative method:**

Graft procedure was adopted for semiquantitative evaluation of the vasoproliferative response of CAM vessels at regular intervals by using stereomicroscope. The score is 0 when no changes can be seen; it is + 1 when few neovessels, and +2 when a considerable change in the number and distribution of the converging neovessels is observed [26].

**Invivo wound healing and angiogenesis:**

The used 60 male albino rats were kept fasting overnight. The dorsal area of each rat was carefully shaved and the skin will disinfect with iodine. The injury was made with some up to 14 mm in diameter [27], following anesthesia with ketamine (dose 60 mg/kg b. wt.) [28]. Just after made of injury, animals were divided into 4 equal groups; 15 animals each. First group was kept as negative non-treated control and Phenytoin was applied for the 2<sup>nd</sup> group. Wounds of 3<sup>rd</sup> and 4<sup>th</sup> group were treated by TiO<sub>2</sub>-NRs 10 µg/ 200 µl and 20 µg/200 µl; respectively. Each group of rate was housed separately. Daily treatment by TiO<sub>2</sub>-NRs solution was applied to the wound bed, Phenytoin was sprayed to the wound bed, while the untreated control group the wound area was washed by a physiological solution. Wound skin samplings (n =2) was conducted on days 0, 3, 5,7,10 and 14, (during which the animals was sacrificed) and collected for analysis [29] and histological examination.

**Histological examination:**

a. The 12<sup>th</sup> day old (7<sup>th</sup> post inoculation) inoculated CAMs were collected from each group in Phosphate Buffered Saline (PBS) pH 7.4 solutions. The membranes tissues were fixed in 10% neutral buffered formalin.

b. Skin samples were fixed in 10% formalin saline, trimmed off, washed and dehydrated in ascending grades of alcohol. The dehydrated specimens were then cleared in xylene, embedded in paraffin blocks and sectioned at 4-6 µm thick.

The prepared tissue sections were deparaffinized using xylol and stained using hematoxylin and eosin (H&E) for histological examination through the electric light microscope [30]. Grading system used in assessing of wound angiogenesis [31].

Score	Histological feature
0	It was given for acellular or rare endothelial cells.
1	It reflected scattered endothelial cells in small groups or linear arrangements but without lumens.
2	Represented endothelial cells in all quadrants of the section, prominent linear arrangements and some tube formation.

3	It was assigned for easily identified capillary tube formation, many containing red blood cells and tiny amounts of collagen.
4	It was reserved for larger vessels that accommodated more than 4 red cells abreast and multilayered vessels containing layers of collagen in vessel walls.

### RESULTS AND DISCUSSION

Yeast was used biosynthesis of TiO<sub>2</sub>-NRs because of the ease of handling, rapid growth, abundant enzyme synthesis [32, 33] and practical storage in the laboratory [34]. Yeast biomasses are capable of producing metal nanoparticles and nanostructures through the reduction of proteins in enzymes either intracellularly or extracellularly [35].

#### FTIR Spectroscopy:

A strong sharp peak at 703 cm<sup>-1</sup> which indicates the presence of TiO<sub>2</sub>-NRs (Fig. 1), the peak at 3421 cm<sup>-1</sup> correspond to OH which is shrunk due to thermal treatment, whereas, the peaks at 2360 cm<sup>-1</sup> and 2338.6 cm<sup>-1</sup> represent the C=H of Albumin egg shells.

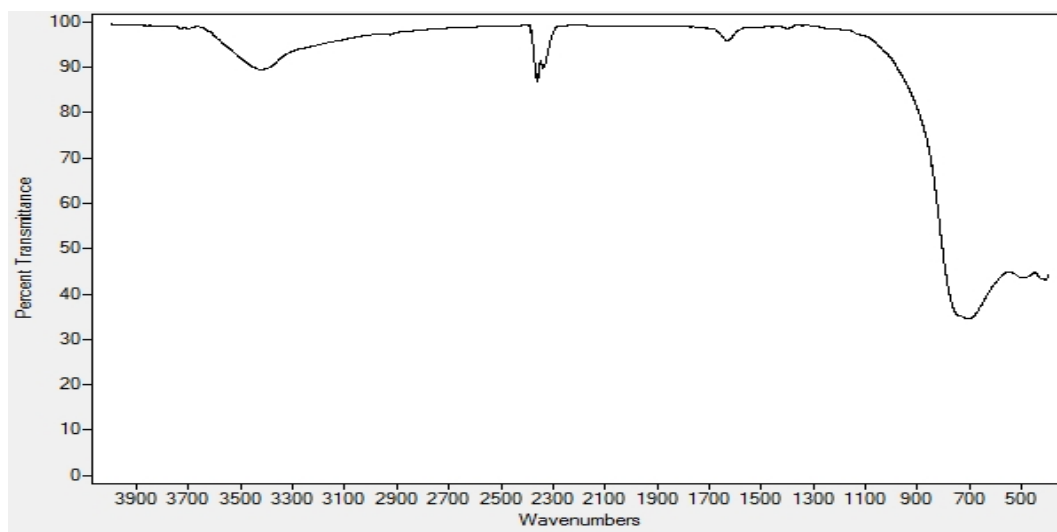


Fig (1). FTIR transmission of TiO<sub>2</sub>-NRs synthesized by yeast as biotemplate.

#### X-ray Diffraction (XRD):

XRD is essential to characterize crystal structure and the crystallinity and confirmed TiO<sub>2</sub> phase [36]. The XRD pattern of TiO<sub>2</sub>-NRs obtained after further thermal treatment under air at 700 °C. The XRD pattern of TiO<sub>2</sub> nanoparticle shows six peaks at 27.4, 36.0, 41.244, 54.332 and 56.598 index to 110,101,111,211,220. It can be seen that the peaks only agree with Rutile phase according to standard (Rutile, JCPDS: 87-0920) [37]. Indicating the high purity and crystallinity obtained for TiO<sub>2</sub> phases. The average crystal sizes of TiO<sub>2</sub>-NRs obtained after calcinations at 700 °C for 90 min confirmed its rod shape with 532 nm length and 244 nm diameter. The average crystallite size (d) of TiO<sub>2</sub>-NRs was estimated by Scherer's equation [36-38]  $d = k\lambda / \beta \cos \theta$

Where k = 0.9 is the shape factor, β is the measured FWHM (Full Width at Half Maximum), θ is the Bragg angle of the peak, λ is the XRD wavelength. The average crystal size of the produced TiO<sub>2</sub>-NRs with calcination at 700 °C for 90 min was found to be 649 nm length and 246 nm diameter (Fig 2).

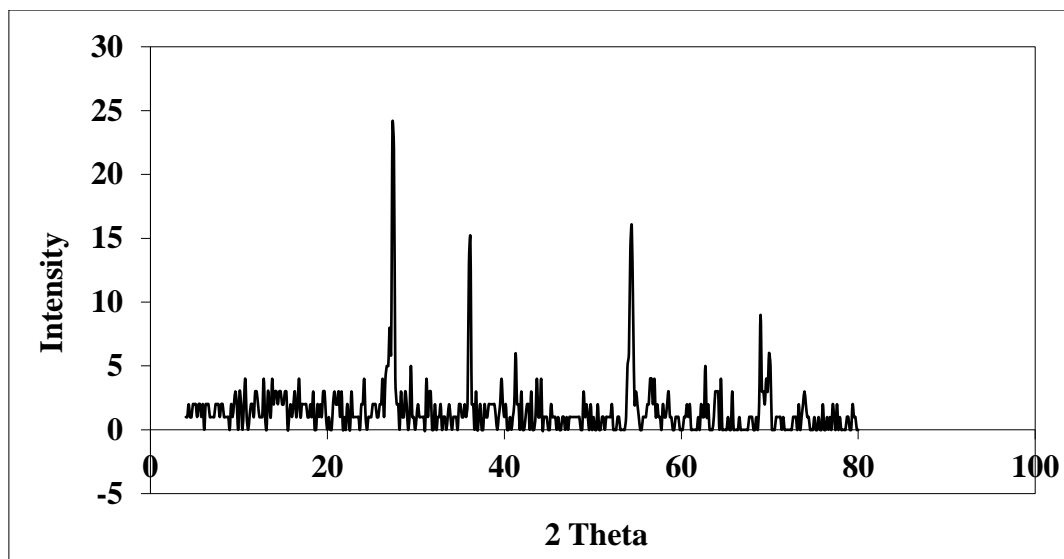


Fig. (2): XRD Pattern of Rutile TiO<sub>2</sub>-NRs synthesized by yeast as biotemplate.

**Morphology studies of TiO<sub>2</sub>-NRs:**

Transmission electron microscopy analyses were carried out to visualize and confirm the morphology, size and structure of the formed crystallites. TEM analysis of TiO<sub>2</sub>-NRs confirmed its rod shape with the dimensions of 244-246 nm length and 532-649 nm diameter, respectively (Fig 3). The obtained results are in agreement with that obtained from the Scherrer equation [36-38].

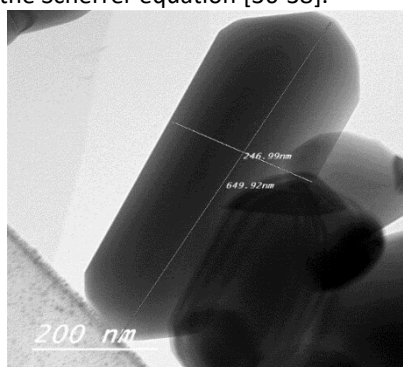
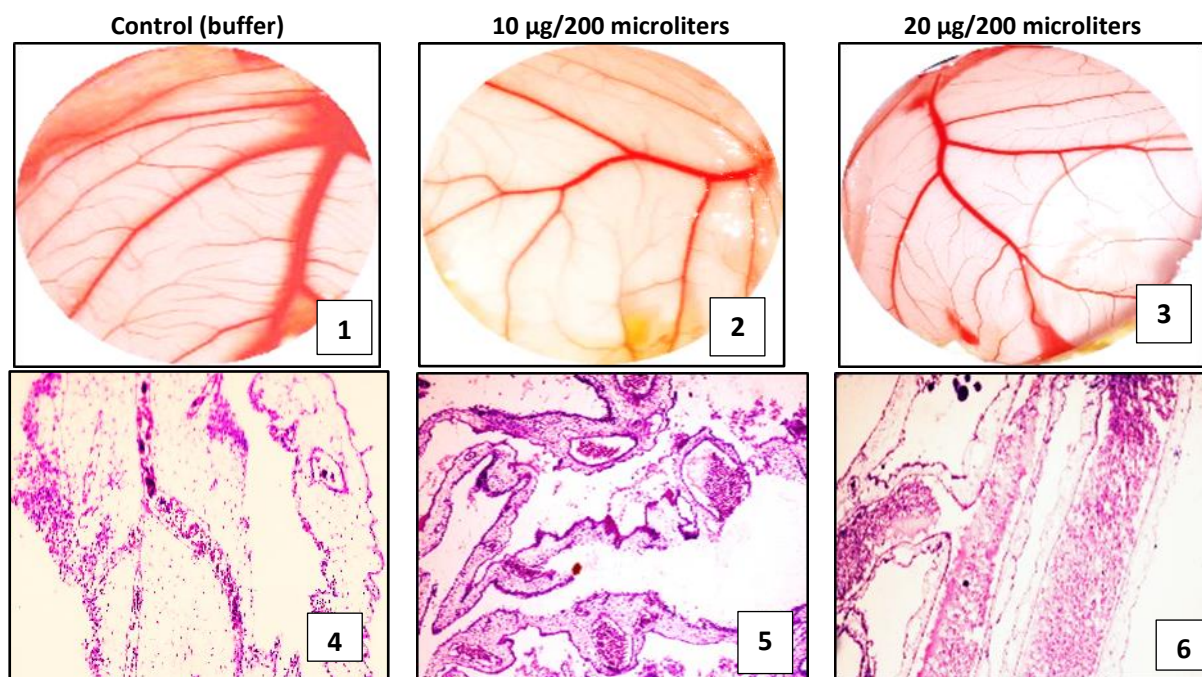


Fig. (3): Transmission electron microscopy of TiO<sub>2</sub>-NRs synthesized by yeast as biotemplate.

**Angiogenesis effect:**

The Angiogenesis effect of TiO<sub>2</sub>-NRs was carried out on chicken embryo CAM [25]. Angiogenesis is defined as a double edged sword and of great importance in various pathological and physiological processes [39-42].





**Fig (4):** Changes in morphology and histology of chicken embryo CAM treated with TiO<sub>2</sub>- NRs in a rate of 10 µg/0.2ml, 20µg/0.2ml or 0.2ml buffer.

Group	TiO <sub>2</sub> µg/200 µgl	
	Control	20
Conc.	Buffer	10
Stereomicroscopic Scoring	0	1
Histopathological Ranking	0	++

**Table (1):** Scoring of CAM angiogenesis and histological findings.

**CAM angiogenesis and histological findings:**

Gross morphology by stereomicroscope and histological examination of control embryonic membranes revealed well defined clear blood vessels containing erythrocytes and appeared as thin branched tubes (Fig 4,1) and score 0 (Table1). Tissue section showed thin well-developed blood islands with vascular branches ranked (0). Gross morphological findings, TiO<sub>2</sub>-NRs using test solutions of angiogenesis at 10 µg/200 microliters demonstrated vascular development in the chick embryo CAM had moderate effect on the formation of blood islands (Fig 4,2) and vascular branching (score 1) (Table1). On other side, TiO<sub>2</sub>-NRs using test solutions of angiogenesis at 20 µg/200 microliters showed blood islands consisted of vascular systems in early embryonic life. CAM revealed considerable increase in the number (Fig 4, 3) and distribution of the more neovessels (score 2) (Table1) as compared with control group. The results prove the activity of TiO<sub>2</sub>-NRs on blood vessels [10,43,44,45] and can explained by high surface energy and microrough surface etopography of Ti substrates promoted the synthesis of pro-angiogenic growth factors, which resulted in an advancement of the human aortic endothelial cells (EC) differentiation in vitro [46], improved neovascularization in vivo [47] and basic fibroblast growth factor (FGF-2) [48].

In hematoxylin and eosin staining tissue sections of (CAM) showed histological findings of normal CAM (Fig 4, 4), new blood vessels with less vascular branching pattern ranked (++) in embryos inoculated with 10 µg (Fig 4, 5) , while 20 µg showed well-developed neovascularization represented by numerous branching patterns of blood vessels. The shape of the main central vessel and distribution of its tree branch pattern ( primary and secondary vessels), crossing of blood vessels, like, sharp turns, bending of vessels, wavy distortions (Fig 4, 6) and random arrangement ranked (+++) (Table1) [44]. Both the visual inspection and histological findings large number of matured blood vessels with highly branched capillary network were observed this view support the angiogenesis activity induced by nanoparticles [6, 45, 49-51].

**Wound healing:**

Wound healing animal models [52] have been developed in small mammals such as rats, mice, and rabbits are relatively inexpensive, require fewer resources, have multiple mutant models for delayed wound healing, and thus are easily obtainable. Furthermore, the wound healing process in small mammals is completed in 1- 2 weeks [53].

**Skin wound angiogenesis:**

Angiogenesis makes critical contribution throughout life with important role in successful regeneration and growth of new tissues [39-40]. Blood vessels provide growing cells and tissues with oxygen and nutrients necessary for survival [41-42]. Regarding angiogenesis in wound during the inflammation phase of wound healing (fig 5) the blood vessels increased in size and branching at the 3<sup>rd</sup> and 5<sup>th</sup> day post excision and treatment ( Fig 5,4-9) as compared with those of 0 times (Fig 5,1-3). Wounds dressed with 20 µg showed prominent vessels and improved neovascularization [47] than 10 µg and Phenytoin spray [45].

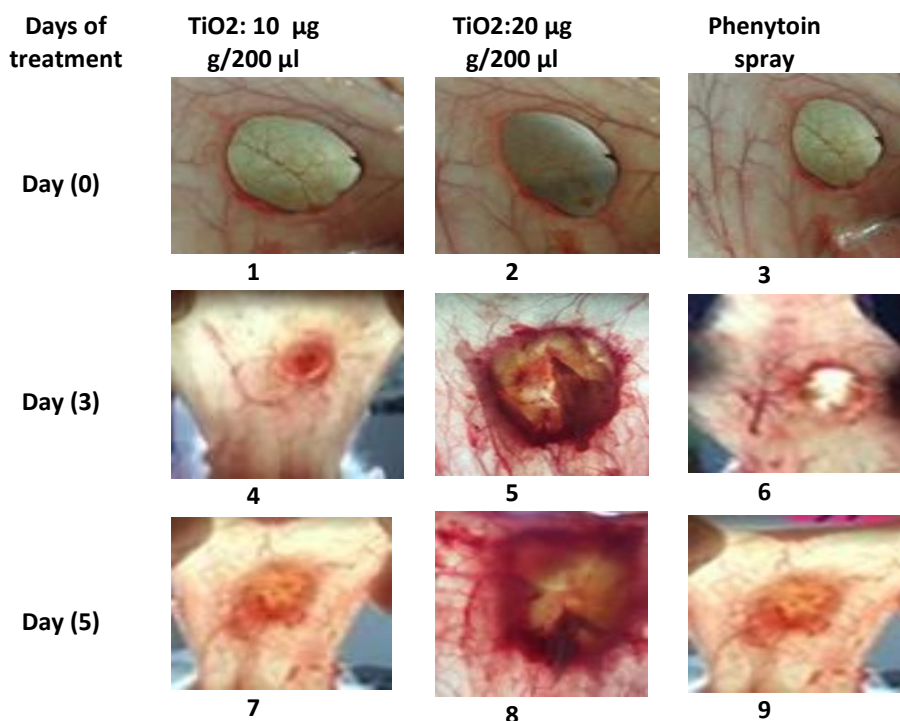


**Fig (5): skin wound angiogenesis of albino rate treated with TiO<sub>2</sub>-NRs in a rate of 10 µg/200 µl, 20µg/200 µl or Phenytoin spray at 0, 3 and 5 days post treatment.**

**Wound morphology:**

Original skin wound is shown in figs (5,1-3). At the 3<sup>rd</sup> day skin wound in animals of untreated, Phenytoin, 10µg/200 µl and 20µg/200 µl groups at the 3<sup>rd</sup> day showed thickening edematous and hotness of epidermis at its cut edges (Figs (5,3-6). At 7 days wound gap was filled with necrotic tissues and inflammatory cell cells ((Fig 5, 10-12). At the 10<sup>th</sup> days after mature granulation tissues filling wound with shrinkage area to 70% of original area.(Fig 5,11-12), while by the 14<sup>th</sup> day wound area in Ti-O<sub>2</sub>-NRs were reduced to 10% (Fig 5, 16 and 17) while Phynatone group was 40% (Fig 5, 18). This result indicated that dressing with Ti-O<sub>2</sub>-NRs accelerate healing of open excision type wounds in vivo [45, 54-56]. Also, Seisenbaeva et al. [57] found that TiO<sub>2</sub> dispersion was the apparently improved regeneration of damaged tissues with appreciable decrease in scar formation and skin color anomalies.



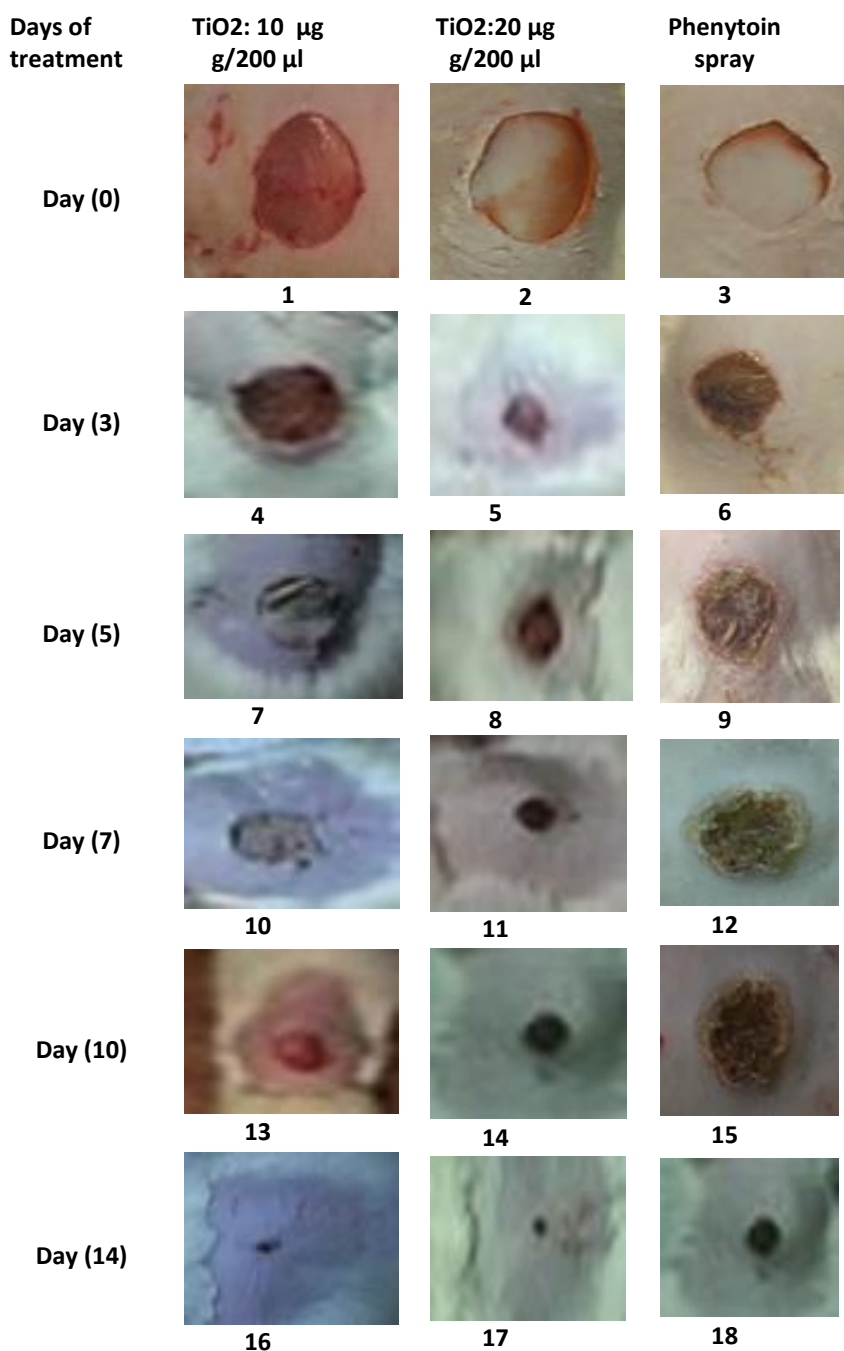


Fig (6): Changes in skin wound morphology of albino rate treated with TiO<sub>2</sub>- NRs in a rate of 10 µg/200 µl, 20µg/200 µl or Phenytoin spray at 0, 3 7,10 and 14 days post treatment

Group No.	Treatment	Score				
		3 days	5 days	7 days	10 days	14 days
1-Control-ve	Untreated	0	0	1	2	3
2-Standard drug	Phenytoin	1	2	2	3	3
3-Treatment	TiO <sub>2</sub> :µg/200 µl	0	1	2	2	3
4-Treatment	TiO <sub>2</sub> :µg/200 µl	1	2	3	3	4

Table (2): scoring of wound angiogenesis.

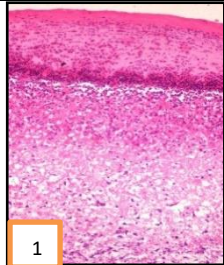
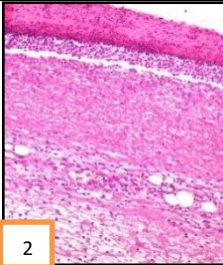
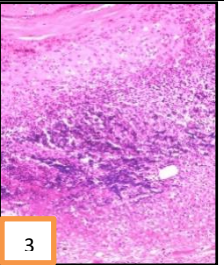
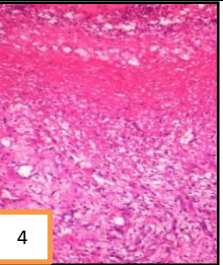
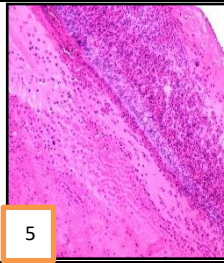
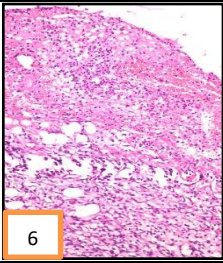
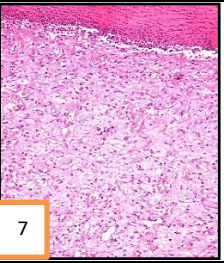
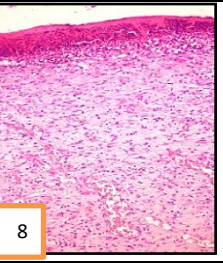
**Histology effect of treatment:**

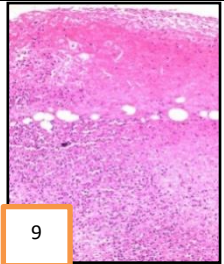
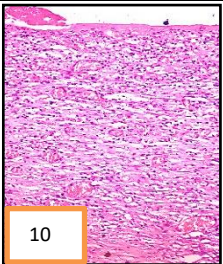
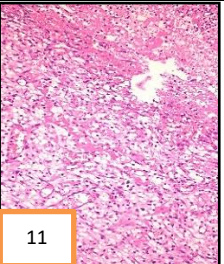
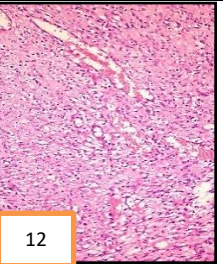
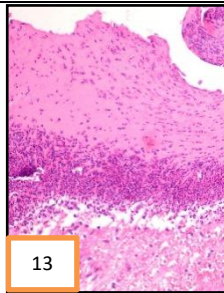
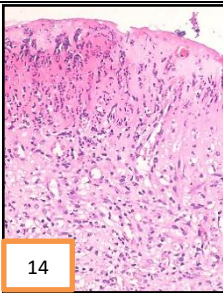
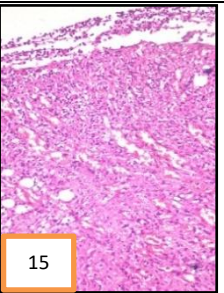
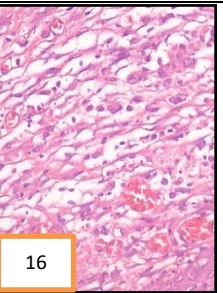
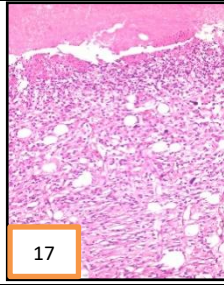
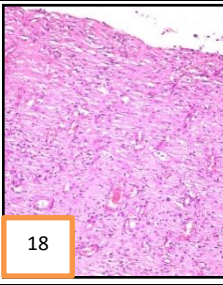
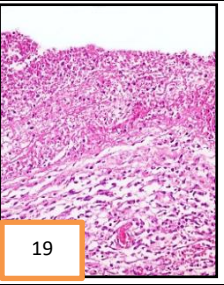
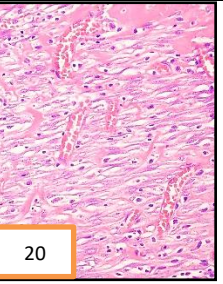
Skin sections of untreated, standard drug, 10µg/200 µl and 20µg/200 µl groups at the 3<sup>rd</sup> day showed that dermis near the excision was rich on inflammatory cells mainly polymorphonuclear cells. The number of fibroblasts absence or mild increased in the dermis near the wounded area. Animal groups of untreated and treated by 10µg/200 µl showed a cellular or rare endothelial cells (score 0) (Table 2, fig.6, 1 and 3). On the other side, the dermal layer displayed the beginning of neo-angiogenesis in Phenytoin or 10µg/200 µl groups (score 1) (Table 2, fig.6, 2 and 4). These finding indicate the start of healing presses.

All examined groups at the 5<sup>th</sup> day of treatment revealed fibrin net rich on inflammatory cells mainly neutrophils, macrophages and lymphocytes. The regeneration of the epidermis was completely inhibited. Mild proliferation and migration of fibroblasts and mild new collagen were observed. Animal control groups showed acellular or rare endothelial cells (Score 0) (Table 2, Fig.6, 5). On the other side, the dermal layer showed the beginning of neo-angiogenesis in standard drug and 20 µg/200 µl treated groups (Score 2) (Table 2) which characterized by prominent linear arrangements and some tube formation (Fig.6, 6 and 8). Animal group treated by 10 µg/200 µl showed scattered endothelial cells in small groups or linear arrangements but without lumens (Score 1) (Table 2, fig.6, 7). These results pointed that treatment accelerate wound healing activity and TiO<sub>2</sub>-NPs are potent [54].

Seven days wound was filled with necrotic tissues and inflammatory cell cells mainly neutrophils in all animal groups. The epidermis regeneration was significantly inhibited. At the bottom of wounds newly created granulation tissue was observed. The granulation tissue consisted of fibroblasts, endothelial cells, and newly synthesized non-organized collagen.

The untreated group revealed scattered endothelial cells in small groups or linear arrangements without lumens (score 1) (Table 2, fig.6, 9). Groups treated with standard drug, and 10 µg/200 µl) showed endothelial cells in all quadrants of the section, prominent linear arrangements and some tube formation (score 2) (Fig.6, 10 and 11). Endothelial cells proliferation are accompanied by new vessels number. It was assigned for easily identified capillary tube formation, many containing red blood cells and tiny amounts of collagen especially in animals treated by 20 µg/200 µl (score 3) (Table 2, fig.12).

Day	Untreated	Stander drug	20 µg g/200 µl	G10 µg g/200 µl
3 Days	 1	 2	 3	 4
	Score: 0	Score: 1	Score: 0	Score: 1
5 Days	 5	 6	 7	 8
	Score: 0	Score: 2	Score: 1	Score: 2

7 Days				
	Score: 1	Score: 2	Score: 2	Score: 3
10 Days				
	Score: 2	Score: 3	Score: 2	Score: 3
14 Days				
	Score: 3	Score: 3	Score: 3	Score: 4

**Fig. (7): Histological findings after treatment of wounds with TiO<sub>2</sub>-NRs.**

At the 10<sup>th</sup> days after wound induction, mature granulation tissues with polymorphonuclear cells infiltration. Animals of untreated group and treated those by 10 µg/200 µl revealed endothelial cells in all quadrants of the section, prominent linear arrangements and some tube formation (score 2) (Table 2, Fig. 13 and 15). On other hand, animal groups treated Phenytoin, and 20 µg/200 µl) showed capillary tube formation, many containing red blood cells and tiny amounts of collagen (score 3) (Table 2, fig.14and 16). By 14 days after wound induction, tissue macrophages predominant from the inflammatory cell's population. The number of fibroblasts and endothelial cells in the granulation tissue decreased and increase of collagen fibers. In case of untreated, Phenytoin and 10 µg/200 µl animals group showed capillary tubes formation which contained red blood cells score (3) (Table 2, fig.6, 17-19). While animals group treated by drug 20 µg/200 µl showed larger vessels that accommodated more than 4 red cells abreast and multilayered vessels containing layers of collagen in vessel walls (score 4) (Fig.20). These histological finding as formation of healthy granulation tissue and re-epithelization indicated the healing progression in treated group [58]. BC-TiO<sub>2</sub> nanocomposite treatment promotes appropriate healing through the fibroblast migration and proper development of epithelial cells along with the restoration of blood supply through the formation of new blood vessels [58]. The wound healing activity of TiO<sub>2</sub>-NPs engineered from a plant *Origanum vulgare* has also been reported in Wistar Albino rats [19]. The biocompatibility and anticoagulant properties of TiO<sub>2</sub>-NPs make them an excellent candidate for wound healing as observed in in vitro and in vivo studies [59]. The results of TiO<sub>2</sub>-based scaffolds revealed the accelerated adhesion, proliferation and differentiation of osteoblasts, and in growth of vascular tissues [59].

The most important result in applying the TiO<sub>2</sub> dispersion was the apparently improved regeneration of damaged tissues, quicker reduction of wound area with appreciable decrease in scar formation and skin color anomalies [17]. The effect of TiO<sub>2</sub> in wound healing can be attributed to its antibacterial activity to



suppress bacteria growth beneath the dressing [60-62], complement activation ability of TiO<sub>2</sub> was reported [64-65], the photocatalytic effect for production of reactive oxygen species to target bacteria in wound infections [66,67].

The obtained results demonstrated that titanium dioxide reduced the time require for wound healing indicated by the faster contraction of the wound treated licorice extract in comparison. With untreated ones .the healing with different concentrations of titanium dioxide extract was significantly higher than untreated group from the second day of treatment until the complete closure of wound. Again titanium dioxide extract was more potent than standard healing agent. Although numerous studies have been done regarding the pharmacological properties of titanium dioxide.

### CONCLUSION

It can be concluded that the wound dressing with TiO<sub>2</sub>-NRs showed promoting effect on wound healing. It is advisable to be used with other medications to cut short the time of wound healing and further investigation has to be done to clarify the exact mechanism of TiO<sub>2</sub>-NRs promotes wound healing.

### Ethical approval

This study was approved from Institutional Animal Ethics Committee and in accordance with local laws and regulations.

### Authors' Contributions:

AMA and HAM designed and planned this study, **AIA**, HAA prepration and characterization of TiO<sub>2</sub>-NRs. MMA and AAE, CAM angiogenesis. M.I. collects tissue samples and histological study. All authors shared samples collection, performing the tests, manuscript writing, drafted , revised the manuscript and approved the final manuscript.

### ACKNOWLEDGMENTS

The authors thank departments of pharmacology and Cytology & Histology, faculty of Vet. Med., Cairo University. Genetic Engineering and Biotechnology Research Institute (GBRI), University of Sadat City, Egypt. College of Biotechnology, Misr University for Science and Technology (MUST), Egypt. Animal Health Research Institute, El-Fayom. El Nasser Company. The authors declared that work was self-funded.

### REFERENCES

- [1] Laurent, D., Forge, M.; Port, A., Roch, C. , Robic, L. and Elst , V. (2008). Magnetic Iron Oxide Nanoparticles: Synthesis, Stabilization, Vectorization, Physicochemical Characterizations, and Biological Applications. *Chem. Rev.*, 108, 2064–2110
- [2] Grande, F, and Tucci, P. (2016). Titanium Dioxide Nanoparticles: a Risk for Human Health? *Mini Rev Med Chem.*, 16(9):762-769.
- [3] Zhang, X., Li, W. and Yang, Z. (2015). Toxicology of nanosized titanium dioxide: an update. *Arch Toxicol.*, 89(12):2207-2217.
- [4] Chen, X. and Mao, S.S. (2007). Titanium dioxide nanomaterials: synthesis, properties, modifications, and applications. *Chemical reviews*, 107(7), 2891-2959.
- [5] Bao, S.j., Lei, C., Xu, M.W., Cai, C. J. and Jia, D. Z. (2012). Environment- friendly biomimetic synthesis of TiO<sub>2</sub> nanomaterials for photocatalytic application. *Nanotechnol.*, 23, 205- 601.
- [6] Ayan, K. B.I, Vimal, V., Sudip, M., Joydeb, M., Ajay, K. P., Sujata, P., Krishnendu, P., Shruthi, M., Rohit, K. R., Suvro, C. and Chitta R. P. (2012). Zinc oxide nanoflowers make new blood vessels. *Nanoscale*, 4, 7861-7869.
- [7] Iavicoli I., Leso V., and Bergamaschi A., 2012. Toxicological Effects of Titanium Dioxide Nanoparticles: A Review of In Vivo Studies. *Journal of Nanomaterials* Volume 2012, Article ID 964381, 36 pages doi:10.1155/2012/964381.

- [8] Ghanbary F. , Seydi E., Naserzadeh P. and Salimi A. (2018). Toxicity of nanotitanium dioxide (TiO<sub>2</sub>-NP) on human monocytes and their mitochondria. *Environmental Science and Pollution Res.*, 25:6739–6750.
- [9] Staton, C.A., Reed, M.W.R. and Brown, N.J. (2009). A critical analysis of current in vitro and in vivo angiogenesis assays. *Int. J. Exp. Pathol.* 90, 195–221.
- [10] Ribatti, D., Nico, B., Vacca, A., Roncali, L., Burri, P.H. and Djonov, V.(2001). Chorioallantoic membrane capillary bed: a useful target for studying angiogenesis and anti-angiogenesis in vivo. *Anat. Rec.* 264, 317–324.
- [11] Vargas, A., Labouebe, M.Z., Lange, N., Gurny, R. and Delie, F. (2007). The chick embryo and its chorioallantoic membrane (CAM) for the in vivo evaluation of drug delivery systems. *Adv. Drug Deliv. Rev.* 59, 1162–1176.
- [12] Spielmann, H., Liebscht, M., Moldenhauer, F., Holzhutter, H.G., Bagley, D.M., Lipman, J.M., Pape, W.J.W., Miltenburger, H., De Silva, O., Hofer, H. and Steiling, W. (1997). CAM-based assays. *Food Chem. Toxicol.* 35, 39–66.
- [13] Alonso, J. E., Lee, J. and Burgess (1996). The management of complex orthopaedic injuries. *Surg Clin North Am* 76: 879
- [14] Lazurus, G., Cooper, M. D., Knighton, D., and Kinl (1994 ). Definitions and guidelines for assessment of wounds and evaluation of healing. *Arch Dermatol.*, 130: 489 – 493.
- [15] Runa, S., Khanal, D., Kemp, M.L. and Payne, C.K. (2016).TiO<sub>2</sub> nanoparticles alter the expression of peroxiredoxin anti-oxidant genes. *J Phys Chem C.* ;120(37):20736–20742. doi: 10.1021/acs.jpcc.6b01939.
- [16] Ahmad, R. and Sardar, M. (2013). TiO<sub>2</sub> nanoparticles as an antibacterial agent against E. coli. *Int J Innov Res Sci Eng Technol.*; 2(8):3569–3574.
- [17] Senarathna U. L. N. H., Fernando S. S. N., Gunasekara T. D. C. P., Weerasekera M. M., Hewageegana H. G. S. P., Arachchi N. D. H., Siriwardena H. D., and Jayaweera P. M.(2017). Enhanced antibacterial activity of TiO<sub>2</sub> nanoparticle surface modified with *Garcinia zeylanica* extract . *Chem Cent J.* 2017; 11: 7. doi: 10.1186/s13065-017-0236-x
- [18] Nakano R., Hara M., Ishiguro H , Yao Y, Ochiai T , Nakata K , Murakami T, Kajioka J , Sunada K, Hashimoto K, Fujishima A and Kubota Y.,( 2013). Broad Spectrum Microbicidal Activity of Photocatalysis by TiO<sub>2</sub>. *Catalysts* , 3(1), 310-323; <https://doi.org/10.3390/catal3010310>
- [19] Sankar, R., Dhivya, R., Shivashangari, K.S. and Ravikumar, V. (2014). Wound healing activity of *Origanum vulgare* engineered titanium dioxide nanoparticles in Wistar Albino rats. *J Mater Sci Mater Med.* Jul;25(7):1701-8. doi: 10.1007/s10856-014-5193-5.
- [20] Muthukumaraswamy, M.G., Sivakumar, G. and Manoharan, G. (1991). Topical Phenytoin in diabetic foot ulcers, *Diabetes Care*, 14: 909-911
- [21] Talas, G., Brown, R.A., and McGruther A. (1999). Role of phenytoin in wound healing-a wound pharmacology perspective, *Biochem Pharmacol*, 57: 1085-1094
- [22] Genever, P.G., Cunliffe, W.J., and Wood, E.J. (1996). Influence of the extracellular matrix on fibroblast responsiveness to phenytoin using in vitro wound healing models, *Br. J. of Dermatol.*, 133:231-235
- [23] Awatef, M. Badrelden, Abd Elmaksoud, I.A. , Dalia Ebeedy, Rana E. Abu El-Maaty, Abeer AB Mohamed and Amr, H. (2017). Green synthesis of silver nanoparticles mediated extract of various in vitro plant (*Bacopa monniri* , *Coleus* , *Blumei* , *Cichrium intybus* . *Bioscience Research.* Vol 15 issues
- [24] Li, Y., Guo, M., Zhang, M. and Wang, X. (2009). Hydrothermal synthesis and characterization of TiO<sub>2</sub> nanorod arrays on glass substrates. *Materials Research Bulletin*, 44 (6) 1232-1237
- [25] Gatne D. P, Mungekar S., Addepalli V., Mohanraj K., Ghone S.A. and Rege N. N. (2016) .Development of collateral vessels: A new paradigm in CAM angiogenesis model. *Microvascular Research*, 103,11–13.
- [26] Ausprunk, D., Knighton, D. and Folkman, J. (1977). Vascularization normal and neoplastic tissues grafted to the chick chorioallantois. *Am. J. Pathol.* 79.597-618\_
- [27] João De Masi, E.C.D. , Campos, A.C. , João De Masi, F.D. , Ratti, M.A ., Ike, I.S. and João De Masi, R.D. (2016). The influence of growth factors on skin wound healing in rats. *Braz J Otorhinolaryngol.* 82(5):512-521.
- [28] Kilkeny, C., Browne, W. J., Cuthill, I. C., Emerson, M. and Altman, D. G. (2010).Improving Bioscience Research Reporting: The Arrive Guidelines for Reporting Animal Research. *PLoS Biol.* 8, e1000412 .



- [29] Kamber, M.; papalazarou, Rouni, Papagerogopoulou, G. papalois, E. and Kostourou ( 2015 ). Angiotensin II inhibitors facilitates epidermal wound regeneration in diabetic mice . *frontiers in physiology* 6 ; 170
- [30] Bancroft, J.D., Stevans, A. and Turner, D.R. (2013): *Theory and practice of histological techniques*. 4th Ed. Churchill Livingstone, Edinburgh, London, Melbourne, New York.
- [31] Hopf, H.W., Gibson, J.J., Angeles, A.P., Constant, J.S., Feng, J.J., Rollins, M.D., Zamiru, I., Hussain, M. and Hunt, T.K. (2005). Hyperoxia and angiogenesis. *Wound Repair Regen*; 13:558–564.
- [32] Kumar, D.; Karthik, L.; Kumar, G. and Roa, K.B. (2011). Biosynthesis of silver nanoparticles from marine yeast and their antimicrobial activity against multidrug resistant pathogens. *Pharmacology online* , 3, 1100–1111.
- [33] Yan, S., He, W., Sun, C., Zhang, X., Zhao, H., Li, Z., Zhou, W., Tian, X., Sun, X. and Han, X. , (2009). The biomimetic synthesis of zinc phosphate nanoparticles. *Dyes Pigment.*, 80, 254–258.
- [34] Dameron, C.T., Reese, R.N., Mehra, R.K., Kortan, A.R., Carroll, P.J., Steigerwald, M.L., Brus, L.E. and Winge, D.R. (1989). Biosynthesis of cadmium sulphid quantum semiconductor crystallites. *Nature*, 338, 596–597.
- [35] Moghaddam B.A., Moniri M., Azizi S., Abdul Rahim R., Bin Ariff A., Saad Z. W., Namvar F., Navaderi M. and Mohamad R. (2017). Biosynthesis of ZnO Nanoparticles by a New *Pichia kudriavzevii* Yeast Strain and Evaluation of Their Antimicrobial and Antioxidant Activities. *Molecules*, 22, 872.
- [36] Cullity, B.D. and Stock, S.R. (2001). *The determination of crystal structure, in elements of X-ray Diffraction*, Prentice Hall, New Jersey, pp. 308-311.
- [37] An, H. R., An, H., Kim, W. B., and Ahn, H. J. (2014). Nitrogen-Doped TiO<sub>2</sub> Nanoparticle-Carbon Nanofiber Composites as a Counter Electrode for Pt-Free Dye-Sensitized Solar Cells. *ECS Solid State Letters*, 3(8), M33-M36.
- [38] Patterson, A.L. (1939). The Scherrer formula for X-ray particle size determination. *Physical review*, 56(10), 978-982 .
- [39] Saghiri, M.A., Asatourian, A., Orangi, J., Sorenson, C. M. and Sheibaniab, N. (2015). Functional role of inorganic trace elements in angiogenesis part I: (N, Fe, Se, P, Au, and Ca). *Crit. Rev. Oncol./Hematol.*, <http://dx.doi.org/10.1016/j.critrevonc.2015.05.010> [Epub ahead of print] Review.
- [40] Saghiri, M.A., Asatourian, A., Orangi, J., Sorenson, C.M. and Sheibani, N. (2015). Functional role of inorganic trace elements in angiogenesis part II: (Cr, Si, Zn, Cu, and S. *Crit. Rev. Oncol./Hematol.*, <http://dx.doi.org/10.1016/j.critrevonc.2015.05.011> [Epub ahead of print] Review.
- [41] Saghiri, M.A., Asatourian, A. and Sheibani, N. (2015). Angiogenesis in regenerative dentistry. *Oral Surg. Oral Med. Oral Pathol. Oral Radiol.* 119, 122.
- [42] Saghiri, M.A., Asatourian, A., Sorenson, C.M. and Sheibani, N. (2015). Role of angiogenesis in endodontics: contributions of stem cells and proangiogenic and antiangiogenic factors to dental pulp regeneration. *J. Endod.* 41, 797–803.
- [43] Melkonian, G., Cheung, L., Marr, R., Tong, C. and Talbot, P. (2002). Mainstream and sidestream cigarette smoke inhibit growth and angiogenesis in the day 5 chick chorioallantoic membrane. *Toxicol. Sci.* 68, 237–248.
- [44] Ejaz, S., Scok, K.B. and Lim, C.W., (2006). A novel model of image acquisition and processing for holistic quantification of angiogenesis disrupted by application of mainstream and side stream cigarette smoke solutions. *Environ. Toxicol. Pharmacol.* 21, 22–33.
- [45] Abd El Maksoud , I. A., Dalia Elbeedy , Hassana A., Amera Hamdy, Osman M. A., Amer M.M., El-Sanousi, A.A. and Aziza M.M. Amer (2018). Studies of Effect of biosynthesized Zinc Oxide Nanospheres (ZnO NSs) on angiogenesis and wound healing. In press
- [46] Raines, A.L., Olivares-Navarrete, R., Wieland, M., Cochran, D.L., Schwartz, Z. and Boyan, B.D. (2010). Regulation of angiogenesis during osseointegration by titanium surface microstructure and energy. *Biomaterials* 31, 4909–4917.
- [47] Schwartz, Z., Raz, P., Zhao, G., Barak, Y., Tauber, M., Yao, H. and Boyan, B. D. (2008). Effect of micrometer-scale roughness of the surface of Ti6Al4V pedicle screws in vitro and in vivo. *J. Bone Joint Surg. Am.* 90, 2485–2498.
- [48] Hurley, M.M., Abreu, C., Gronowicz, G., Kawaguchi, H. and Lorenzo, J. (1994). Expression and regulation of basic fibroblast growth factor mRNA levels in mouse osteoblastic MC3T3-E1 cells. *J. Biol. Chem.* 269, 9392–9396.

- [49] Patra C. R., Bhattacharya R., Patra S., Vlahakis N. E., Gabashvili A., Koltypin Y., Gedanken A., Mukherjee P. and Mukhopadhyay D., 2008. Pro-angiogenic Properties of Europium(III) Hydroxide Nanorods *Adv. Mater.*, 20(4), 753–756.
- [50] Augustine R., Dominic E. A., Reju I., Kaimal B. and Kalarikkal N. (2014). Investigation of angiogenesis and its mechanism using zinc oxide nanoparticle-loaded electrospun tissue engineering scaffolds. *RSC Adv.*, 4, 51528-51536.
- [51] . Ahtzaza S., Nasira M., Shahzadia L., Amirb W., Anjumb A., Arshadb R., Iqbala F., Chaudhrya A. A., MuhammadY. and Rehman I., 2017. A study on the effect of zinc oxide and zinc peroxide nanoparticles to enhance angiogenesis-pro-angiogenic grafts for tissue regeneration applications. *Material and Design*, 132, 409-418.
- [52] Kim, D. J., Mustoe, T. and Clark, R. A. (2015). Cutaneous wound healing in aging small mammals: a systematic review. *Wound Repair Regen.* 23, 318–339. doi:10.1111/wrr.12290
- [53] Dorsett-Martin, W. A., Wysocki, A. B. (2008). Rat models of skin wound healing, in *Sourcebook of Models for Biomedical Research*, ed. P. M. Conn (Totowa, NJ: Humana Press), 631–638.
- [54] Peng, C. C. , Yang, M.H., Wen-Ta Chiu ,W.T., Chiu, C.H., Yang, C. S. , Chen, Y.W., Chen, K.C. and Peng, R.Y. (2008) .Composite nano-titanium oxide-chitosan artificial skin exhibits strong wound-healing effect-an approach with anti-inflammatory and bactericidal kinetics. *Macromol. Biosci.* 8, 316–327 .
- [55] Archana, D., Singh, B.K. and Dutta, J. (2013). In vivo evaluation of chitosan-PVP-titanium dioxide nanocomposite as wound dressing material. *Carbohydr Polym.*, 95(1):530-539.
- [56] Archana, D., Singh, B.K. and Dutta, J. (2015). Chitosan-PVP-nano silver oxide wound dressing: in vitro and in vivo evaluation. *Int J Biol Macromol.*, 73: 49-57.
- [57] Seisenbaeva G.A, Fromell K., Vinogradov V.V., Terekhov A. N., Pakhomov A. V., Nilsson B., Ekdahl K.N., Vinogradov V. V. and Kessler V. G. (2017). Dispersion of TiO<sub>2</sub> nanoparticles improves burn wound healing and tissue regeneration through specific interaction with blood serum proteins. *Scientific Reports* | 7: 15448 | DOI:10.1038/s41598-017-15792-w
- [58] Khalid, A., Ullah, H., Ul-Islam, M., Khan, R., Khan, S., Fi Ahmad, F., Khan, T. and Wahid, F. (2017). Bacterial cellulose-TiO<sub>2</sub> nanocomposites promote healing and tissue regeneration in burn mice model. *RSC Adv.*, 7, 47662
- [59] Wu, J. Y., Li, C. W. , Tsai, C. H., Chou ,C. W., Chen, D. R. , Wang, G. J., *Nanomed. Nanotech. Biol. Med.*, 2014, 10(5), 1097–1107.
- [60] Feng, B., Weng J. , Yang, B.C., X.Qu S.X. and Zhang , D. (2003). Characterization of surface oxide films on titanium and adhesion of osteoblast. *Biomaterials*, 24:4663-4670.
- [61] Ovington, L.G. *Advances in wound dressings.* *Clin Dermatol*, 2007; 25:33-38.
- [62] Tsai, T.T., Sung, W.P. Song, W. (2011). Identification of Indoor Airborne Microorganisms and Their Disinfection with Combined Nano-Ag/TiO<sub>2</sub> Photocatalyst and Ultraviolet Light. *Environ Eng Sci*, 28:635-642.
- [63] Walivaara, B., Askendal, A., Lundstrom, I. , Tengvall, P. (1996). Blood protein interactions with titanium surfaces. *Journal of Biomaterials Science-Polymer Edition* 8, 41-48.
- [64] Tengvall, P. (2001). in *Titanium in Medicine.* (eds. D.M. Brunette, P. Tengvall, M. Textor & P. Thomsen) pp457-485 (Springer-Verlag Berlin Heidelberg, Berlin, Germany).
- [65] Tengvall, P. , Askendal, A. (2001). Ellipsometric in vitro studies on blood plasma and serum adsorption to zirconium. *J. Biomed. Mater. Res.* 57, 285-290.
- [66] Hershey, R.A. (2010). Development of titania nanofibers and films for the mitigation of wound infection. *Theses and Dissertations.* 862. <http://utdr.utoledo.edu/theses-dissertations/86> .
- [67] Azad, A. M., Aboelzahab, A. , Goel, V. (2012). Bactericidal and wound disinfection efficacy of nanostructured titania. *Adv. Mater. Res.* 1, 309–345.